Influence of magnon-phonon coupling on the phonon dynamics of one-dimensional antiferromagnets

M. Malard and A. S. T. Pires
Departamento de Física, Universidade Federal de Minas Gerais, 30123-970 Belo Horizonte, Brazil
(Received 18 April 2007; revised manuscript received 15 June 2007; published 10 September 2007)

The interplay between magnetic and elastic degrees of freedom, the so-called magnon-phonon coupling, plays an important role in magnetism. The Green's function technique is used to investigate the phonon dynamics for the one-dimensional antiferromagnet with $S=1$ within the framework of an interaction Heisenberg model. This is treated via the Holstein-Primakoff transformation in the context of the modified spin-wave theory. The obtained phonon's relaxation function provides a measure of the effect of magnon-phonon coupling on phonon energy and lifetime.

DOI: 10.1103/PhysRevB.76.104407 PACS number(s): 75.10.Jm, 75.10.Pq, 75.40.Gb

I. INTRODUCTION

In the last years, a considerable attention has been devoted to the study of magnetic systems with vibrational degrees of freedom. That has been stimulated by the belief that magnon-phonon interaction can be the relevant mechanism behind a variety of frontier problems, both in theoretical and experimental physics.[1–4]

The existence of an excitation gap and a finite correlation length in one-dimensional integer spin antiferromagnets is, by now, well established theoretically, numerically, and experimentally. This effort has been mostly motivated by the phenomenological difference that the emerging gap fixed between integer and half-integer antiferromagnetic (AFM) spin chains. The gapless spin-1/2 case was settled some time before integer systems were first studied.[5–7] The low dimensional spin-1 antiferromagnets in the presence of external fields, with anisotropies and dimerization, are now abundantly addressed in the literature.[8] However, as Anderson[9] pointed out, on top of all the preceding interactions, the frustration of the spin lattice can be caused by lattice fluctuations coupled to the spin system as well. Indeed, from first principles, it was shown that the nontrivial ground states of certain quasi-one-dimensional magnets, which have been generally accepted as due to competing FM and AFM exchanges only, depend also on the interaction between magnons and phonons.[10] Recent experimental works support this hypothesis.[1,2,11–13]

Yet, the dynamics of spin-1 AFM chains coupled to phonons has not been sufficiently explored. It is well known that the spin-1/2 AFM chain coupled to phonons develops a spin gap via the dimerization of the lattice. This is known as the spin-Peierls effect.[14] The phonon driven one-dimensional *XY* model undergoes spin-Peierls transition too and has been approached in different ways. The method of Mori was applied by Pires,[15] a random-phase approximation was preferred by Holicki *et al.*,[16] and the renormalization group method by Sun *et al.*[17] Although Schulz[18] has shown that we cannot expect a spin-Peierls instability for an integer spin chain, we believe that the effects due to the magnon-phonon coupling play an important role for the dynamics of such systems. This is the subject of the present paper.

For two-dimensional magnets, the study of magnon-phonon coupling has been carried out in various forms. The Green's function technique has been applied within the machinery of the ferromagnetic Heisenberg background[19–21] as well as in the *s-d* model.[22] The two-dimensional AFM Hamiltonian has been addressed as well.[3,4] In the classical scenario, the phonon dynamics for a compressible Heisenberg chain was investigated about 27 years ago by Fivez *et al.*[23,24] through the continued-fraction approximation.

The present work can be justified both theoretically and experimentally. Besides adding to the conceptual background of magnetoelastic phenomena in low-dimensional magnets, it also helps in the understanding of the new behaviors revealed by many recent materials. High-temperature superconductivity is probably the most prominent example in this scenario,[25] once it has become well known that the AFM Heisenberg model provides a suitable effective hamiltonian for the cuprate superconductors.[4]

In Sec. II, an interaction Hamiltonian is provided by the one-dimensional AFM Heisenberg model with position dependent exchange. It is handled through Holstein-Primakoff transformations in the context of modified spin-wave theory.[26] In Sec. III, the phonon Green's functions are calculated to second order in the coupling, as well as the corresponding self-energies. In Sec. IV, the acoustic and optical phonon relaxation functions are given. The phonon energy and lifetime, as modified by the coupling with magnons, are discussed. Our conclusions are presented in Sec. V.

II. MODEL

The interaction between elastic and magnetic degrees of freedom is carried out by explicating the exchange integral dependence on the magnetic site positions. Consider the one-dimensional isotropic Heisenberg Hamiltonian with nearest-neighbor AFM exchange. Written in two sublattices, as suitable for the AFM case, with appropriate boundary periodic conditions, it splits like $H=H_s+H_{sp}$, where

$$H_s = \frac{J}{2}\sum_{i=1}^{N} \vec{S}_{i-1}\cdot\vec{T}_i + \vec{T}_i\cdot\vec{S}_{i+1}, \tag{1}$$

$$H_{sp} = \frac{\alpha}{2}\sum_{i=1}^{N} (y_i - x_{i-1})\vec{S}_{i-1}\cdot\vec{T}_i + (x_{i+1} - y_i)\vec{T}_i\cdot\vec{S}_{i+1}, \tag{2}$$

with $\vec{S}_i$, x_i and $\vec{T}_i$, y_i denoting spin operators and position displacement operators from different sublattices A and B.

We also have N denoting the number of sites, $J=J(a)$ for the exchange integral evaluated at the lattice parameter a, and $\alpha=\frac{dJ}{dr_{ij}}|_{r_{ij}=a}$, where r_{ij} is the distance between two magnetic sites. H_s is the usual spin Hamiltonian for interacting AFM excitations and H_{sp}, the "spin-phonon" Hamiltonian, corresponds to AFM excitations interacting with each other and with the phonons.

A satisfactory AFM solution for the unperturbed Hamiltonian H_s, given in Eq. (1), cannot be obtained through a naive spin-wave theory. It is well known that the usual Holstein-Primakoff or Dyson-Maleev expansions about an ordered state are not adequate to treat low-dimensional AFM Heisenberg models.

The modified spin-wave (MSW) theory of Takahashi for low-dimensional magnets[26] brings about the AFM disordered ground state through the explicit imposition of zero sublattice magnetization. In fact, using a variational density matrix approach, the Mermim-Wagner theorem[27] is enforced by hand; MSW theory does not display rotational invariance naturally. Arovas and Auerbach,[28] using the Schwinger boson representation, proposed a more rigorous, rotationally invariant theory for low-dimensional AFM systems, reaching final results in equivalence to those of Takahashi. MSW theory is also analogous to the approach of Hirsch and Tang,[29] corresponding to the one-loop static correction for the dressed magnon frequency in the Green's function, when the magnon-magnon interaction is taken into account. Finally, MSW theory agrees with numerical results and has been used in two dimensions even for $S=1/2$. A more detailed discussion on the approximation and its validities can be found in Ref. 28.

Specializing to the case of our interest, the unperturbed $D=1$ and $S=1$ antiferromagnets were solved by Pires and Gouvea[30] using Dyson-Maleev transformations (Holstein-Primakoff plus other two magnon processes allowed) within the framework of MSW theory. The approximation amounts to calculate the static effect of the interaction between magnons up to second order, obtaining an effective system of free magnons with renormalized masses. Higher order terms were neglected based on low-temperature arguments. Following the authors' procedure and references cited therein, the Hamiltonian H_s is written in terms of Bogoliubov magnon creation and annihilation operators as

$$H_m=\sum_q \hbar\omega_q^m(\alpha_q^\dagger\alpha_q+\beta_q^\dagger\beta_q), \tag{3}$$

where we have replaced the subscript s for "spin" of Eq. (1) by m for "magnon," indicating that, after Dyson-Maleev transformation, the Hamiltonian represents bosonlike magnetic excitations, the magnons. In Eq. (3), $\omega_q^m=\lambda(1-[\eta\cos(qa)]^2)^{1/2}$ is the renormalized (dressed) magnon frequency predicted by the method. The coefficients used to rotate the operators in the Bogoliubov transformations are written in terms of a function θ_q which, for the one-dimensional (1D) MSW theory, obeys $\tanh(2\theta_q)=-\eta\cos(qa)$. The parameters λ and η are obtained self-consistently. The other relevant static quantity obtained by Pires and Gouvea for the above model was the gap as a function of temperature [Eqs. (12a) and (12b) in their paper[30]]. In particular, at $T=0$, the gap decreases as $e^{-\pi S}$, in accordance with the $O(3)$ nonlinear sigma model prediction [Eq. (11) and the following discussion[30]]. We remark that no symmetry has been broken in this solution and the problem remains fully SU(2).

Now, let H_p be the phonon Hamiltonian, written accordingly in two sublattices as

$$H_p=\frac{1}{2}\sum_{i=1}^{N}\frac{m}{2}(\dot{x}_{i-1}^2+\dot{y}_i^2)+\frac{k}{2}[(y_i-x_{i-1})^2+(x_{i+1}-y_i)^2]. \tag{4}$$

Diagonalized Hamiltonian H_p, written in terms of phonon creation and annihilation operators, reads

$$H_p=\sum_q \hbar\omega_q^{ap}\left(c_q^\dagger c_q+\frac{1}{2}\right)+\hbar\omega_q^{op}\left(d_q^\dagger d_q+\frac{1}{2}\right). \tag{5}$$

It splits into two parts associated with acoustic and optical free phonons with frequencies given by $\omega_q^{ap}=c[1-\cos(2qa)]^{1/2}$ and $\omega_q^{op}=c[1+\cos(2qa)]^{1/2}$, where $c=\sqrt{2\kappa/m}$; κ is the elastic constant and m is the magnetic ion mass.

The total Hamiltonian which takes into account the full degrees of freedom of the magnetoelastic system is $H_t=H_0+H_{sp}$, with $H_0=H_s+H_p$ being the unperturbed Hamiltonian for the lattice. The ground state of this additive Hamiltonian is the product of the individual phonon and magnon ground states: $|0\rangle=|0\rangle_s|0\rangle_p$, where $|0\rangle_s$ is the magnon vacuum state and $|0\rangle_p$ is the phonon vacuum state. In order to study the influence of the interaction Hamiltonian on this state, we submit H_{sp} to the following technology.

We introduce the Holstein-Primakoff transformation to write the spin operators in terms of magnon operators as

$$S_i^+=S_i^x+iS_i^y=\sqrt{2S}a_i,\quad S_i^-=S_i^x-iS_i^y=\sqrt{2S}a_i^\dagger,\quad S_i^z=S-a_i^\dagger a_i, \tag{6}$$

$$T_i^+=T_i^x+iT_i^y=\sqrt{2S}b_i^\dagger,\ T_i^-=T_i^x-iT_i^y=\sqrt{2S}b_i,\ T_i^z=-S+b_i^\dagger b_i. \tag{7}$$

Then, we transform to collective coordinates

$$a_l=\frac{1}{\sqrt{N/2}}\sum_q a_q e^{-iql},\quad b_l=\frac{1}{\sqrt{N/2}}\sum_q b_q e^{+iql},$$

$$x_l=\frac{1}{\sqrt{N/2}}\sum_q x_q e^{-iql},\quad y_l=\frac{1}{\sqrt{N/2}}\sum_q y_q e^{-iql}, \tag{8}$$

with $q=2\pi n/N$, $n=0,\ldots,N/2$, and redefine the position operators as

$$x_q=\frac{1}{\sqrt{2}}(\xi_q+\eta_q),\quad y_q=\frac{1}{\sqrt{2}}(\xi_q-\eta_q). \tag{9}$$

Finally, we apply the usual Bogoliubov transformations upon the magnon operators,

$$a_q = u_q \alpha_q + v_q \beta_q^\dagger, \quad b_q = v_q \alpha_q^\dagger + u_q \beta_q, \tag{10}$$

where $u_q = \cosh \theta_q$ and $v_q = \sinh \theta_q$, for a given function θ_q, such that $u_q^2 - v_q^2 = 1$.

After the above algebra, the interaction Hamiltonian reads

$$H_{mp} = h_1^\xi + h_2^\xi + h_1^\eta + h_2^\eta, \tag{11}$$

$$h_1^\xi = \sum_{q,k} M_1(q,k) \xi_q (\alpha_{k+q}^\dagger \alpha_k + \beta_{k+q} \beta_k^\dagger),$$

$$h_2^\xi = \sum_{q,k} M_2(q,k) \xi_q (\alpha_{k+q}^\dagger \beta_k^\dagger + \beta_{k+q} \alpha_k), \tag{12}$$

$$h_1^\eta = \sum_{q,k} N_1(q,k) \eta_q (\alpha_{k+q}^\dagger \alpha_k - \beta_{k+q} \beta_k^\dagger),$$

$$h_2^\eta = \sum_{q,k} N_2(q,k) \eta_q (\alpha_{k+q}^\dagger \beta_k^\dagger - \beta_{k+q} \alpha_k), \tag{13}$$

where the coefficients M and N are given in Appendix A. We have replaced the subscript sp for "spin-phonon," in the interaction Hamiltonian by mp for "magnon-phonon," indicating that, after Holstein-Primakoff transformation, the evolving interaction is between phonons and magnons. In writing Eqs. (12) and (13), we have neglected terms containing four magnon operators once the effect of interest here is the interaction between magnons and phonons such that the secondary interaction between magnons can be disregarded. This overall negligence of two magnon processes in H_{mp} is also the reason why we started with Holstein-Primakoff instead of Dyson-Maleev transformations for the spin operators. The interaction [Eq. (11)] acts upon $H_0 = H_s + H_p$ ground state $|0\rangle = |0\rangle_s |0\rangle_p$.

III. PHONON GREEN'S FUNCTION AND SELF-ENERGY

In the interaction representation, the acoustic and optical phonon Green's functions are expanded in powers of H_{mp}. In terms of operators ξ_q and η_q, they read[31]

$$D^{ap}(q;t,t') = \frac{2m\omega_q^{ap}}{\hbar} \sum_{n=0}^{\infty} \frac{(-i)^{n+1}}{n!} \int dt_1 \cdots \int dt_n \frac{\langle 0|T\hat{\xi}_q(t)\hat{\xi}_{-q}(t')\hat{H}_{mp}(t_1)\cdots\hat{H}_{mp}(t_n)|0\rangle}{\langle 0|S(\infty,-\infty)|0\rangle}, \tag{14}$$

$$D^{op}(q;t,t') = \frac{2m\omega_q^{op}}{\hbar} \sum_{n=0}^{\infty} \frac{(-i)^{n+1}}{n!} \int dt_1 \cdots \int dt_n \frac{\langle 0|T\hat{\eta}_q(t)\hat{\eta}_{-q}(t')\hat{H}_{mp}(t_1)\cdots\hat{H}_{mp}(t_n)|0\rangle}{\langle 0|S(\infty,-\infty)|0\rangle}, \tag{15}$$

where T is the time-ordering operator, $S(t,t') = e^{iH_0 t/\hbar} e^{-iH(t-t')/\hbar} e^{-iH_0 t'/\hbar}$ is the S matrix for the problem and $\hat{O}(t) = \exp(iH_0 t/\hbar) O \exp(-iH_0 t/\hbar)$. The term $n!\langle 0|S(\infty, -\infty)|0\rangle$ accounts for the normalization of the Green's function expansion. Because of the linearity of the interactions [Eqs. (12) and (13)] in ξ or η, all the odd contributions to Eqs. (14) and (15) correspond to brackets with an odd number of phonon operators and thus vanish.

After Fourier transforming, the zeroth order (unperturbed) phonon Green's functions read

$$D_0^{ap}(q,\omega) = \frac{1}{\sqrt{2\pi}} \frac{2\omega_q^{ap}}{\omega^2 - \omega_q^{ap\,2}}, \quad D_0^{op}(q,\omega) = \frac{1}{\sqrt{2\pi}} \frac{2\omega_q^{op}}{\omega^2 - \omega_q^{op\,2}}. \tag{16}$$

For higher orders, we will need the unperturbed magnon Green's function. It is convenient to define (for operators α and β)

$$G_0^\alpha(q,t-t')\delta_{q',q} = -i\langle 0|T\hat{\alpha}_q(t)\hat{\alpha}_{q'}^\dagger(t')|0\rangle,$$

$$G_0^\beta(q,t-t')\delta_{q',q} = -i\langle 0|T\hat{\beta}_q(t)\hat{\beta}_{q'}^\dagger(t')|0\rangle, \tag{17}$$

$$\tilde{G}_0^\alpha(q,t-t')\delta_{q',q} = -i\langle 0|T\hat{\alpha}_q^\dagger(t)\hat{\alpha}_{q'}(t')|0\rangle,$$

$$\tilde{G}_0^\beta(q,t-t')\delta_{q',q} = -i\langle 0|T\hat{\beta}_q^\dagger(t)\hat{\beta}_{q'}(t')|0\rangle. \tag{18}$$

After Fourier transforming,

$$G_0^{\alpha/\beta}(q,\omega) = \frac{1}{\sqrt{2\pi}} \frac{1}{\omega - \omega_q^m}, \quad \tilde{G}_0^{\alpha/\beta}(q,\omega) = \frac{1}{\sqrt{2\pi}} \frac{-1}{\omega + \omega_q^m}. \tag{19}$$

Now, for the second-order contribution, we apply Wick's theorem for writing the brackets via the Feynman diagram technique. Collecting only the different and connected diagrams,[33] this contribution for the phonon Green's function accounts for diagrams of the form

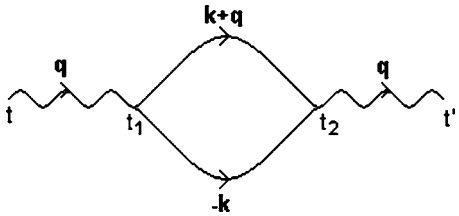

The curly lines represent the unperturbed phonon Green's function (acoustic or optical depending on the case), while the smooth ones stand for the unperturbed magnon Green's function (of type α or β).

Green's functions at finite temperatures are obtained following the development of Matsubara, as presented in the book of Mahan.[31] Written to second order through Dyson equation, the temperature dependent phonon Green's functions read

$$D_2(q,w) = D_0(q,w) + D_0(q,w)\Sigma_2(q,w)D_0(q,w), \quad (20)$$

where the second-order self-energies are given by

$$\Sigma_2(q,\omega) = \Sigma_2'(q,\omega) + i\Sigma_2''(q,\omega), \quad (21)$$

$$\Sigma_2'(q,\omega) = P\int_0^\pi \frac{dk}{\pi}\left[\frac{A(q,k)}{\omega-\Omega_+(q,k)} - \frac{A(q,k)}{\omega+\Omega_+(q,k)} + \frac{B(q,k)}{\omega-\Omega_-(q,k)} - \frac{B(q,k)}{\omega+\Omega_-(q,k)}\right], \quad (22)$$

$$\Sigma_2''(q,\omega) = -\pi\sum_i \int_0^\pi \frac{dk}{\pi}[d_+(q,k_{i+}^+)A(q,k)\delta(k-k_{i+}^+) + d_+(q,k_{i+}^-)A(q,k)\delta(k-k_{i+}^-) + d_-(q,k_{i-}^+)B(q,k)\delta(k-k_{i-}^+) + d_-(q,k_{i-}^-)B(q,k)\delta(k-k_{i-}^-)]. \quad (23)$$

For simplicity of notation, in the above equations for the acoustic and optical phonon Green's functions and self-energies, we have dropped the corresponding superscripts *ap* and *op*. The functions $A(q,k)$ and $B(q,k)$ are given in the Appendix B for the acoustic and optical cases. They depend on temperature via the magnon occupation number $n_k^m = [\exp(\beta\omega_k^m)-1]^{-1}$ with $\beta = 1/k_BT$. In Eq. (22), we have $\Omega_\pm(q,k) = \omega_k^m \pm \omega_{k+q}^m$. In Eq. (23), $d_\pm(q,x) = \left[\frac{\partial\Omega_\pm(q,k)}{\partial k}\Big|_{k=x}\right]^{-1}$; $k_{i\pm}^+$ and $k_{i\pm}^-$ are, respectively, the roots of $\omega+\Omega_\pm(q,k)=0$ and $\omega-\Omega_\pm(q,k)=0$, for a given q. In both equations, $\int_0^\pi \frac{dk}{\pi}$ stands for the original Σ_k, where $k = \frac{2\pi n}{N}$ for $n=0,\ldots,N/2$. For given values of the variables q and w and the model parameters, the phonon self-energy real and imaginary parts are numerically obtained.

IV. PHONON RELAXATION FUNCTION, FREQUENCY, AND LINEWIDTH

We use the known relation for the relaxation function in terms of the Green's function imaginary part,[31]

$$R(q,\omega) = -\frac{1}{\pi\omega}D''(q,\omega), \quad (24)$$

to obtain an expression in terms of the calculated self-energies,

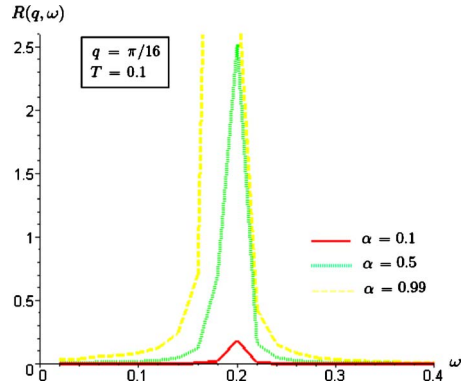

FIG. 1. (Color online) Acoustic phonon relaxation functions versus frequency for $q=\pi/16$, $T=0.1$, and three coupling constant values $\alpha=0.1,0.5,0.99$.

$$R(q,\omega) = -\frac{1}{\pi\omega}\left(\frac{2\omega_q}{\sqrt{2\pi}}\right)^2 \times \frac{\Sigma''(q,\omega)}{\left[\omega^2-\omega_q^2-\frac{2\omega_q}{\sqrt{2\pi}}\Sigma'(q,\omega)\right]^2+\left[\frac{2\omega_q}{\sqrt{2\pi}}\Sigma''(q,\omega)\right]^2}. \quad (25)$$

The above expression applies for both the acoustic and optical cases with the corresponding phonon frequencies and second-order self-energies.

The peak position of the relaxation function gives the phonon frequency, or energy, whose shift from the zero coupling value ω_q is measured by the self-energy real part. To a good approximation, it can be given by the expression $\tilde{\omega}_q^2 = \omega_q^2 + \frac{2\omega_q}{\sqrt{2\pi}}\Sigma'(q,\omega_q)$. The relaxation function linewidth is associated with the phonon damping, or its inverse lifetime, arising from the magnon-phonon coupling; its behavior is governed by the self-energy imaginary part. For the same approximation, it becomes $\Gamma_q = \frac{2\omega_q}{\sqrt{2\pi}}\Sigma''(q,\omega_q)$. For the investigation of the phonon dynamics under the operation of the magnon-phonon coupling, we look to the relaxation function together with its squared peak position and linewidth in three cases: (i) for fixed q and T and varying α, (ii) for fixed q and α and varying T, and (iii) for fixed α and T and varying q.

Hereafter, we will consider q and α as dimensionless parameters through proper unit transformations and letting $J=a=1$. Also, T is made dimensionless when measured in terms of J through the convention $k_B=1$.

A. Acoustic phonons

Figure 1 shows the acoustic phonon relaxation function $R(q,\omega)$ versus frequency ω for $q=\pi/16$, $T=0.1$, and three coupling constant values $\alpha=0.1,0.5,0.99$. We restricted to $\alpha<1$ for our perturbative method for the Green's function presumes a small coupling constant to make sense. As we can see, the peak position shifts slightly to the left together with an enlargement of the linewidth with increasing coupling constant. Indeed, in Fig. 2 for $\tilde{\omega}_q^2(\alpha)$ versus α, it is manifested that the stronger the magnon-phonon interaction, the smaller the phonon energy. This suggests that the inter-

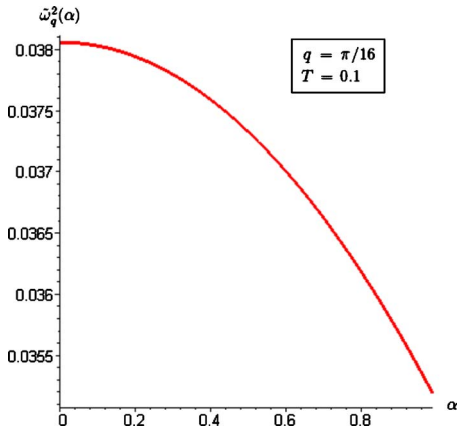

FIG. 2. (Color online) Squared acoustic phonon energy versus coupling constant for $q=\pi/16$ and $T=0.1$.

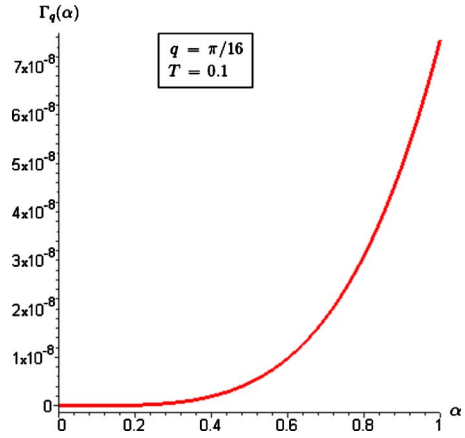

FIG. 3. (Color online) Acoustic phonon linewidth versus coupling constant for $q=\pi/16$ and $T=0.1$.

action tends to transfer energy from the elastic to the magnetic degrees of freedom. In the absence of the magnon-phonon coupling, the phonon energy acquires its full value of $\omega_{\pi/16}=0.195\,09$ for the relative typical values $\kappa=1$, $m=4$, and $a=1$, as reproduced by the $\alpha=0$ graphical value. This direction of energy transfer envisages the magnon-phonon coupling as a source of disorder for the magnetic background. In fact, more energetic magnons correspond to smaller spin-spin correlation length. In what concerns the spin-1 AFM chain disordered ground state, the proper quantity for comparison with magnons is the phonon energy as a function of α for $q=T=0$. The qualitative behavior of such a curve is analogous to that observed for the quite small values $q=\pi/16$ and $T=0.1$: magnon-phonon coupling also enhances the primitive magnetic disorder. A complementary result to the phonon energy dependence on α is provided in Ref. 8, where the effect of magnon-phonon coupling on the Haldane gap was studied for AFM spin-1 Heinsenberg chains. The authors have found the Haldane gap as an increasing function of the coupling, thus subscribing the direction of the energy transfer in the considered systems. Continuing the curve beyond our data, $\tilde{\omega}_q^2$ will vanish for a finite value of α (>1), suggesting the occurrence of a system instability at this point. We remark that this is not physical but a spurious behavior of our perturbative method when the expansion parameter α exceeds 1. As mentioned above, the perturbative theory is not supposed to work for this regime of coupling constant. In fact, for noncritical 1D $S=1$ AFM systems, we expect $\tilde{\omega}_q^2 \to 0$ when $\alpha \to \infty$ in a smooth way. Figure 3 for $\Gamma_q(\alpha)$ versus α evidences that the phonon damping does increase with stronger interaction. It is expected that the interaction shortens the phonon's lifetime, accelerating its decay. When $\alpha=0$, the damping vanishes, in agreement with the elastic background of coupled harmonic oscillators leading to free phonons with infinite lifetime. However, this must not be the case in a real system where, besides the magnon-phonon coupling, other mechanisms, such as electron-phonon coupling and phonon anharmonic interactions, also contribute to damping.

Figure 4 shows the acoustic phonon relaxation function $R(q,\omega)$ versus frequency ω for $q=\pi/16$, $\alpha=0.1$, and three temperature values $T=0.1, 0.145, 0.195$. For this choice of values, we have numerically obtained the temperature dependent parameters λ and η, following the self-consistent equations of Takahashi[26] in the $1DS=1$ AFM background. The peak position does not seem to be sensitive to temperature changes in the range considered. The linewidth clearly grows with temperature. Figure 5 for $\tilde{\omega}_q^2(T)$ versus T shows an increase of the phonon energy with temperature. Actually, this is reasonable that the system's gain in thermal energy due to increasing temperature be shared amongst the phonons. Though conforming with qualitative expectations, the variation of the phonon energy with temperature is quantitatively small, as can bee seen in the vertical graph scale. That is why, in Fig. 4, the shifts on the relaxation function peaks were imperceptible. This very modest dependence with temperature is due to the level of approximation we have used in our model. Had we gone farther in the perturbation series for the Green's function, the thermal contribution to the phonon energy should had been greater. Nevertheless, our second-order approximation captures the main qualitative thermal behavior of the system, that is, the loss in the phonon energy due to the coupling with magnons shrinks in the face of strong thermal activity. Increasing temperature beyond our

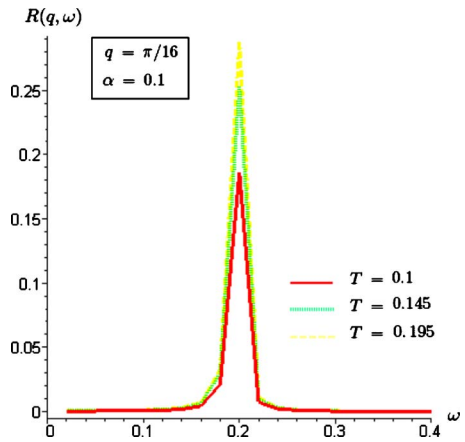

FIG. 4. (Color online) Acoustic phonon relaxation functions versus frequency for $q=\pi/16$, $\alpha=0.1$, and three temperature values $T=0.1, 0.145, 0.195$.

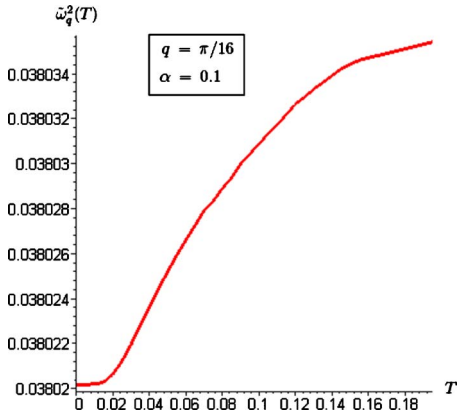

FIG. 5. (Color online) Squared acoustic phonon energy versus temperature for $q=\pi/16$ and $\alpha=0.1$.

data, the $\tilde{\omega}^2_{\pi/16}$ zero coupling value of 0.038 06 will eventually be restored and then surpassed. Figure 6 for $\Gamma_q(T)$ versus T shows that the phonon damping remains equal to 0 until $T=0.04$ and then begins to grow almost linearly with temperature. That is to say, for higher temperatures, where the system's fluctuations get stronger, the role of the spin dynamics in shortening the phonon lifetimes is more significant. Again, the curve passing through the origin is a "nonphysical" characteristic of the harmonic model. The value of $\pi/16$ for q in the above situations was so chosen because the phonons measured in Raman experiments often have small but nonzero wave vectors.[32]

Figure 7 shows the acoustic phonon relaxation function $R(q,\omega)$ versus frequency ω for $\alpha=0.1$, $T=0.1$, and three wave vector values $q=1.1755, \pi/2, 1.9661$. The reason for the choice of $\pi/2$ will become clear soon. The other values were chosen to be equidistant from $\pi/2$. The peak position is maximum for the intermediate value of $\pi/2$ and coincides for the equidistant q values. The linewidth behavior is not so conspicuous by this graph. Figure 8 for $\tilde{\omega}_q^2$ versus q shows the usual form for the (squared) phonon dispersion law. It seems not to be much affected by the coupling with magnons. However, the accurate viewer will observe a very tiny dip located near $q=\pi/2$. In Fig. 9, we plotted $\tilde{\omega}_q^2$ for α

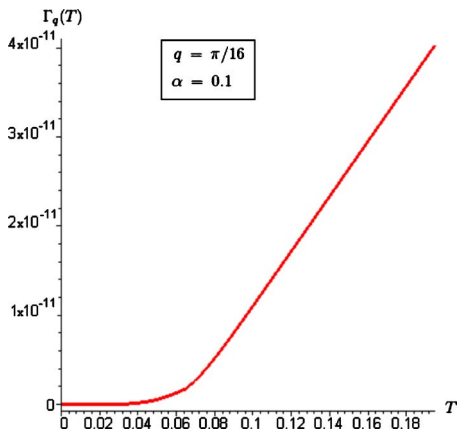

FIG. 6. (Color online) Acoustic phonon linewidth versus temperature for $q=\pi/16$ and $\alpha=0.1$.

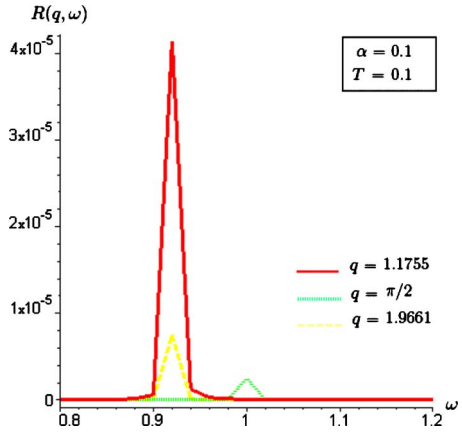

FIG. 7. (Color online) Acoustic phonon relaxation functions versus frequency for $\alpha=0.1$, $T=0.1$, and three wave vector values $q=1.1755$, $\pi/2, 1.9661$.

$=0.1$ and $\alpha=0$. Indeed, for $\alpha=0.1$ (and $T=0.1$), there is a preferential region of wave vectors, around the middle Brillouin zone, where the magnon-phonon coupling transfers energy from the elastic to the magnetic background. Far from $q=\pi/2$, phonon frequencies do not fit the energy change of any possible magnon transition. In principle, for stronger coupling, less energetic phonons start to participate in the interactions with magnons. Figure 10 for Γ_q versus q shows that the damping increases linearly with q in the small q region, reaching a maximum near $q=0.2$ and then drops rapidly to zero. There is another very low weight peak near $q=2.0$ but it is so small that it does not scale with the $q=0.2$ one. The occurrence of well-separated peaks is due to the gap in the magnon energy spectrum. This shows that the phonon lifetime is strongly q dependent, the decay being more drastic for small wave vector phonons.

Finally, comparing the phonon linewidth magnitudes with those of energies, we see that we have $\Gamma/\tilde{\omega} \ll 1$ for the three cases, indicating well-defined phonon excitations for all considered ranges of parameters.

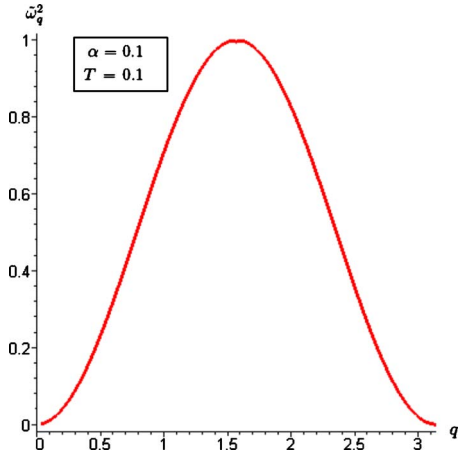

FIG. 8. (Color online) Squared acoustic phonon energy versus q for $\alpha=0.1$ and $T=0.1$.

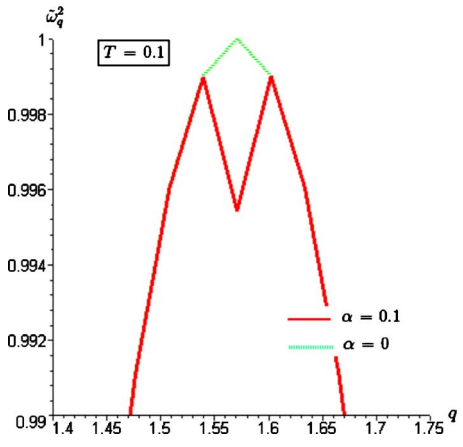

FIG. 9. (Color online) Squared acoustic phonon energies versus q for $T=0.1$ and two coupling constant values $\alpha=0,0.1$.

B. Optical phonons

The dependences on the coupling constant and temperature of the optical phonon energy and linewidth are analogous to those already discussed for acoustic phonons. The energy decreases with stronger coupling and grows with temperature. The linewidth grows both with the coupling and temperature.

For the optical phonon energy dependence on q, we found the same dip at $q=\pi/2$ as in the acoustic case. Figure 11, zooming in the middle Brillouin zone, shows a comparative graph for the (squared) acoustic and optical phonon dispersion laws $\tilde{\omega}_q^2$ for $\alpha=0.1$ and $T=0.1$. The dip in the acoustic curve is followed by the same change in the optical one. By joining the complementary acoustic and optical branches defined in the reduced zone, one gets a gapless and symmetric phonon spectrum in the entire zone, as must be for equal masses coupled by equal stiffness springs. The optical linewidth dependence on q is shown in Fig. 12 for Γ_q. The main peak occurs around $q=2.5$, i.e., different from the acoustic case, optical phonons have stronger finite lifetime effects in the large wave vector region. By the vertical scales of the acoustic and optical phonon linewidths, it is apparent that the damping caused by the coupling with magnons is a hundred

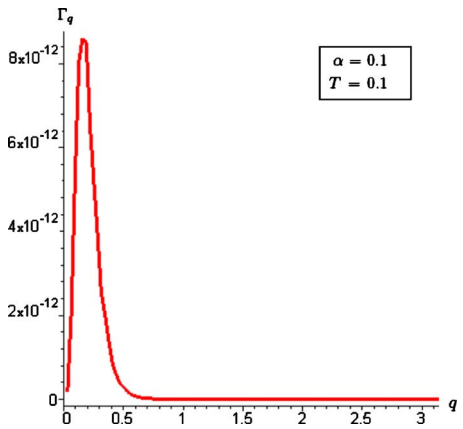

FIG. 10. (Color online) Acoustic phonon linewidth versus q for $\alpha=0.1$ and $T=0.1$.

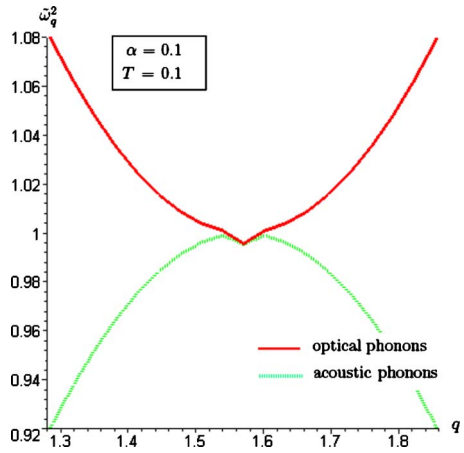

FIG. 11. (Color online) Squared optical and acoustic phonon energies versus q for $\alpha=0.1$ and $T=0.1$.

times stronger for the optical mode. Two tiny lateral peaks are also detectable in Fig. 12, one slightly to the right of the main peak and the other, more far apart, in the small q region. These additional peaks are due to the gap in the magnon energy spectrum.

V. CONCLUSIONS

We have derived the coupling between magnons and phonons in an $S=1$ AFM elastic chain by means of a Heisenberg interaction model, within the framework of the modified spin-wave theory. We have dealt with two magnon and one phonon processes emerging from a second-order Green's function expansion. The acoustic and optical phonon relaxation functions have been obtained from the corresponding self-energy real and imaginary parts.

The dependences of the phonon energy and linewidth on coupling, temperature, and wave vector have been investigated. The results indicate that the coupling tends to transfer energy from the elastic to the magnetic degrees of freedom and to abbreviate the phonon lifetime. At elevated temperatures, thermal activity tends to pump energy in the phonons while squeezing their decay. The phonon dynamics under the

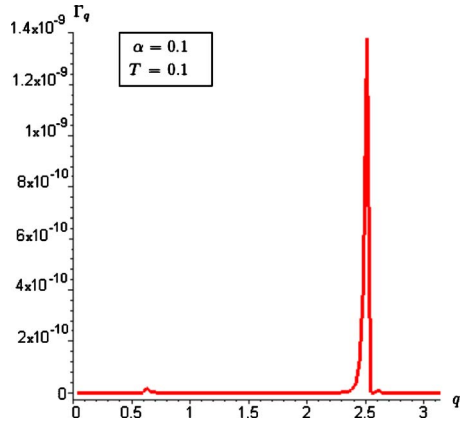

FIG. 12. (Color online) Optical phonon linewidth versus q for $\alpha=0.1$ and $T=0.1$.

coupling with magnons is strongly q dependent. In the phonon dispersion law, the primary region to be affected by the coupling is the middle Brillouin zone. The main peak of the acoustic phonon linewidth is in the small q region, while for optical phonons it is located in the large q region.

From the above collection of results, the phonon energy as a decreasing function of the coupling is the one exposing the magnon-phonon interaction as a source of spin frustration. In Summary, 1D spin-1 AFM elastic system enjoys nonthermal fluctuations, engendered by the magnon-phonon coupling, that decidedly favor the magnetic disorder. This complete quantum effect, which professedly plays an important role in other systems of recent interest, can be observed under the phonon dynamics point of view that we have accomplished.

Our results can be compared with neutron or x-ray scattering on compounds which can realize a $1D$ $S=1$ antiferromagnetic structure, through fitting experimental data with the theoretical relaxation function (or, equivalently, the dynamic structure factor). However, as far as we know, there are no such experimental results available in the literature for these systems. We hope that this work can stimulate experimentalists to check the present theoretical predictions.

ACKNOWLEDGMENT

This work was partially supported by CNPq, Brazil.

APPENDIX A

$$M_1(q,k) = i\frac{2\alpha S}{\sqrt{N}}\sin\left(\frac{q}{2}\right)\left[\cos\left(\frac{q}{2}\right)\cosh(\theta_k+\theta_{k+q}) + \cos\left(k+\frac{q}{2}\right)\sinh(\theta_k+\theta_{k+q})\right],$$

$$M_2(q,k) = i\frac{2\alpha S}{\sqrt{N}}\sin\left(\frac{q}{2}\right)\left[\cos\left(\frac{q}{2}\right)\sinh(\theta_k+\theta_{k+q}) + \cos\left(k+\frac{q}{2}\right)\cosh(\theta_k+\theta_{k+q})\right],$$

$$N_1(q,k) = i\frac{2\alpha S}{\sqrt{N}}\cos\left(\frac{q}{2}\right)\left[\sin\left(\frac{q}{2}\right)\cosh(\theta_k-\theta_{k+q}) + \sin\left(k+\frac{q}{2}\right)\sinh(\theta_k-\theta_{k+q})\right],$$

$$N_2(q,k) = i\frac{2\alpha S}{\sqrt{N}}\cos\left(\frac{q}{2}\right)\left[\sin\left(\frac{q}{2}\right)\sinh(\theta_k-\theta_{k+q}) + \sin\left(k+\frac{q}{2}\right)\cosh(\theta_k-\theta_{k+q})\right]$$

APPENDIX B

$$A^a(q,k) = +\frac{\sqrt{(2\pi)\hbar}}{2m\omega_q^{ap}}M_2(q,k)M_2(-q,k+q)(n_k^m+n_{k+q}^m+1),$$

$$B^a(q,k) = -\frac{\sqrt{(2\pi)\hbar}}{2m\omega_q^{ap}}M_1(q,k)M_1(-q,k+q)(n_k^m-n_{k+q}^m),$$

$$A^o(q,k) = -\frac{\sqrt{(2\pi)\hbar}}{2m\omega_q^{op}}N_2(q,k)N_2(-q,k+q)(n_k^m+n_{k+q}^m+1),$$

$$B^o(q,k) = -\frac{\sqrt{(2\pi)\hbar}}{2m\omega_q^{op}}N_1(q,k)N_1(-q,k+q)(n_k^m-n_{k+q}^m).$$

[1] T. Rudolf, Ch. Kant, F. Mayr, J. Hemberger, V. Tsurkan, and A. Loidl, New J. Phys. **9**, 76 (2007).
[2] T. Rudolf, Ch. Kant, F. Mayr, J. Hemberger, V. Tsurkan, and A. Loidl, Phys. Rev. B **75**, 052410 (2007).
[3] X. Su and H. Zheng, Solid State Commun. **109**, 323 (1999).
[4] X. B. Wang, J. X. Li, Q. Jiang, Z. H. Zhang, and D. C. Tian, Phys. Rev. B **50**, 7056 (1994).
[5] H. A. Bethe, Z. Phys. **71**, 205 (1931).
[6] P. Jordan and E. Wigner, Z. Phys. **47**, 631 (1928).
[7] I. Affleck, J. Phys. A **31**, 4573 (1998).
[8] M. E. Gouvea and A. S. T. Pires, Phys. Rev. B **75**, 052401 (2007) and references cited therein.
[9] P. W. Anderson, Science **235**, 1196 (1987).
[10] C. J. Fennie and K. M. Rabe, Phys. Rev. Lett. **96**, 205505 (2006).
[11] J. Hemberger, T. Rudolf, H. A. Krug von Nidda, F. Mayr, A. Pimenov, V. Tsurkan, and A. Loidl, Phys. Rev. Lett. **97**, 087204 (2006).
[12] K. Y. Choi, V. P. Gnezdilov, P. Lemmens, L. Capogna, M. R. Johnson, M. Sofin, A. Maljuk, M. Jansen, and B. Keimer, Phys. Rev. B **73**, 094409 (2006).
[13] A. B. Sushkov, O. Tchernyshyov, W. Ratcliff, S. W. Cheong, and H. D. Drew, Phys. Rev. Lett. **94**, 137202 (2005).
[14] E. Pytte, Phys. Rev. B **10**, 4637 (1974).
[15] A. S. T. Pires, Solid State Commun. **129**, 621 (2004).
[16] M. Holicki, H. Fehske, and R. Werner, Phys. Rev. B **63**, 174417 (2001).
[17] P. Sun, D. Schmeltzer, and A. R. Bishop, Phys. Rev. B **62**, 11308 (2000).
[18] H. J. Schulz, Phys. Rev. B **34**, 6372 (1986).
[19] T.-M. Cheng, L. Li, and X. Ze, Solid State Commun. **141**, 89 (2007).
[20] T.-M. Cheng, L. Li, and X. Ze, Phys. Lett. A **353**, 431 (2006).
[21] L. M. Woods, Phys. Rev. B **65**, 011409 (2001).
[22] J. M. Wesselinowa, J. Magn. Magn. Mater. **279**, 276 (2004).
[23] J. Fivez, B. De Raedt, and H. De Raedt, J. Phys. C **14**, 2923 (1981).
[24] J. Fivez, H. De Raedt and B. De Raedt, Phys. Rev. B **21**, 5330 (1980).
[25] T. Jarlborg, arXiv:cond-mat/0508672v1 (unpublished).

[26] M. Takahashi, Phys. Rev. B **40**, 2494 (1989).
[27] N. D. Mermin and H. Wagner, Phys. Rev. Lett. **17**, 1133 (1966).
[28] D. P. Arovas and A. Auerbach, Phys. Rev. B **38**, 316 (1988).
[29] J. E. Hirsch and S. Tang, Phys. Rev. B **40**, 4769 (1989).
[30] A. S. T. Pires and M. E. Gouvea, J. Magn. Magn. Mater. **241**, 315 (2002).
[31] G. D. Mahan, *Many-Particle Physics* (Plenun, New York, 1981).
[32] K. F. McCarty, H. B. Radousky, J. Z. Liu, and R. N. Shelton, Phys. Rev. B **43**, 13751 (1991).
[33] The vacuum polarization diagrams generated by the S matrix exactly cancel the disconnected terms, while $n!$ cancels the repeated ones.